

## DEVELOPMENT AND CHARACTERIZATION OF *CITRUS LIMON*-PHOSPHOLIPID COMPLEX AS AN EFFECTIVE PHYTOCONSTITUENT DELIVERY SYSTEM

PRACHI P. UDAPURKAR\*, OMPRAKASH G. BHUSNURE,  
SANTOSH R. KAMBLE

*School of Pharmacy, Swami Ramanand Teerth Marathwada University, Nanded, 431 606, (MS) India*

### ABSTRACT

The aim of the present study is to develop a complex of standardized *Citrus Limon* extract (SCL) and phospholipid with a goal to improve the bioavailability of its phytoconstituents. Diosmin is a flavonoid glycoside, present in *Citrus Limon* known to possess various therapeutic properties. The poor solubility and dissolution rate limit its oral absorption and bioavailability. The phospholipid-SCL complex was prepared using solvent evaporation method and characterized by various parameters like solubility studies, particle size determination, infrared absorption (FTIR), Differential scanning calorimetry (DSC), X-ray diffraction (XRD), Scanning electron microscopy (SEM), entrapment efficiency etc. SEM and XRD reveal the reduction in crystallinity of extract in the complex. FTIR and DSC confirm the formation of phyto-phospholipid complex. The *in vitro* dissolution studies revealed a significantly higher efficiency of complex in releasing the SCL in comparison to the pure SCL, or the physical mixture. Phospholipid complex of SCL may be of potential use in increasing the permeability and hence the bioavailability of diosmin. The result of the study revealed that the phospholipid complex may be considered as a promising drug delivery system that improves the absorption and bioavailability of plant constituents.

**KEYWORDS:** *Standardized Citrus Limon extract, diosmin, phospholipids, characterization, and Citrus phytosome.*

### INTRODUCTION

*Citrus Limon* is an important medicinal plant and is cultivated all over the world of the family Rutaceae. *C. Limon* fruit extract contains many active ingredients such as total flavonoids, (flavones, flavanones), pectins, ascorbic acid, hesperidin and diosmin.<sup>1</sup> Citrus flavonoids have a large spectrum of biological activity including antibacterial, antifungal, antidiabetic, anticancer and antiviral.<sup>2-6</sup> Citrus is frequently used in popular medicine, and over the past two decades their potential therapeutic properties have been largely investigated by *in vitro* and *in vivo* assays. Different experimental studies support the beneficial effects of dietary citrus against many diseases, such as cardiovascular, neurodegenerative pathologies and cancer, due to the high content of polyphenols.<sup>7</sup> The flavonoid composition of *Citrus Limon* extract contains flavanones (Eriocitrin, Hesperidin); Flavones (6, 8-di-C-Glu-Apigenin, 6, 8-di-C-Glu-Diosmetin, 7-O-Rut-Luteolin, Diosmin); Aglycones (Luteolin).<sup>8</sup>

Flavonoids can function as direct antioxidants and free radical scavengers, and have the capacity to modulate enzymatic activities and also inhibit cell proliferation. In plants, flavonoids play a defensive role against invading pathogens, such as bacteria, fungi and viruses. The chemical structures and physicochemical properties of flavonoids justify their rate and extent of absorption.<sup>9</sup> The biological activities of flavonoids and other phytoconstituents depend on their bioavailability. Very little information is available about bioavailability of flavonoids; they are generally present in glycosylated forms in plants.<sup>10</sup> The therapeutic uses of bioconstituents are very popular for health maintenance by various means.<sup>11</sup> Diosmin is flavonoid glycoside present in citrus plant or derived from the flavonoid hesperidin.<sup>12</sup> Diosmin is considered to be a vascular-protecting agent used to help improving chronic venous insufficiency (CVI), hemorrhoids, lymphedema, and varicose veins.<sup>13-14</sup> Phytosome is a technique where plant polyphenolics are complexes with phospholipids to

improve bioavailability of phytoconstituents.<sup>15-20</sup> Phospholipids play a major role as a carrier for molecules requiring sustained release and stability against microbial degradation *in vivo*. They form stable and bioavailable amphiphilic drug lipid complexes with reduced interfacial tension between the system and the GI fluid; thereby facilitating the membrane permeability of the drug.<sup>21</sup> Phospholipids are lipid molecules where glycerol is bonded to two fatty acids. Phospholipids, mainly phosphatidylcholine, are lipophilic substances and readily form complex with polyphenolic compounds. Phosphatidylcholine is a major structural constituent of all biological membranes. Phosphatidylcholine is a major component of soybean lecithin which provides free choline in the blood for the manufacture of acetylcholine; regulates digestive, cardiovascular and liver functions.<sup>22-24</sup> Several other studies have indicated the beneficial role of phospholipids in increasing the therapeutic efficacy of some bioactive phytoconstituents having poor oral absorption such as naringenin, catechin, embelin, and extracts like green tea and grape seed.<sup>25</sup> The primary aim of the present study was to evaluate the feasibility of improving solubility of standardized *Citrus Limon* extract (SCL) by preparing its vesicular complex with phosphatidylcholine. This complex is referred in this paper as Citrus Phytosome (CP). Considering the additive and synergistic effect of various constituents, the whole extract standardized to the content of diosmin was used for formulation rather than only diosmin. CP was prepared using a solvent evaporation method. The formulation and the process variables for the preparation of the CP were optimized using a Quality by design (QbD) approach. Response surface analysis by the means of central composite design was employed for the optimization of the critical process parameters (CPP) on the SCL entrapment rate of CP. The prepared CP were characterized physicochemically for chemical interaction (FT-IR), thermal analysis

(DSC), crystallinity (X-RPD) surface morphology (SEM), solubility and dissolution rate study.

## MATERIALS AND METHODS

### Materials

Standardized extract of *Citrus Limon* was obtained as a gift sample from Kisalaya herbals Pvt. Ltd., Indore. Diosmin was purchased from Sigma Aldrich, Mumbai (India). Phosphatidylcholine was purchased from Ozone international, Mumbai. All other chemicals and reagents were of analytical grade.

### Preparation of Citrus Phytosome (CP)

The CP was prepared by refluxing followed by solvent evaporation technique.<sup>26</sup> CP was prepared in different ratios, i.e., 0.5:1, 0.75:1, 1:1, 2.5:1 and 3:1 of Phosphatidylcholine to SCL. Phosphatidylcholine and SCL were dissolved in dichloromethane and Methanol respectively. Both the solutions were mixed and pour in a 200 ml round bottomed flask. The mixture was refluxed for different duration i.e. 1-4 hr and at various temperature 45-65°C. The resulting clear solution was evaporated and dried under vacuum (40°C). The residues were then gathered and stored in desiccators for further use.

### Quality by Design-based Design of Experiment

A QbD-based approach using a central composite design to obtain a response surface design was employed to systematically study the combined influence of the formulation and process variables such as the phospholipids-drug ratio ( $X_1$ , w/w), the reaction temperature ( $X_2$ , °C), and the reaction time ( $X_3$ , h) on the critical quality attributes (CQAs) of the product i.e., the entrapment efficiency. Using this design, the influence of three factors was evaluated, and the experimental trials were carried out at all 20 possible combinations.<sup>27-28</sup> A statistical model incorporating interactive and polynomial terms was used to evaluate the response employing the equation:

$$Y = b_0 + b_1X_1 + b_2X_2 + b_3X_3 + b_4X_1^2 + b_5X_2^2 + b_6X_3^2 + b_7X_1X_2 + b_8X_1X_3 + b_9X_2X_3$$

Where Y is the dependent variable,  $b_0$  is the intercept representing arithmetic mean response of the 20 runs, and  $b_1$  to  $b_9$  is the estimated coefficient for the factor ( $X_i$ ,  $i=1,2,3$ ).  $X_1$ ,  $X_2$ , and  $X_3$  are the coded levels of independent variables. The interaction terms ( $X_1X_2$ ,  $X_2X_3$ , and  $X_1X_3$ ) showed how the response changes when all three factors

were simultaneously changed. The polynomial terms ( $X_1^2$ ,  $X_2^2$ , and  $X_3^2$ ) were included to investigate nonlinearity. The level values of the three factors, the real values of the central composite design batches, and the resulting entrapment efficiencies are shown in Tables 1 and 2.

**Table 1**  
*Coded Level and Real Values for each Factor under Study*

Variables	Levels				
	-1.68	-1	0	1	1.68
X1	0.5	1.0	1.75	2.5	3.0
X2	45	50	55	60	65
X3	1	1.5	2	2.5	3.0

### **Characterization of CP**

#### **Apparent Solubility of CP**

The apparent solubility was determined by adding excess of extract and CP to 5 ml of water or n-octanol in sealed glass containers at room temperature (25-30°C). The liquids was agitated for 24 hours then centrifuged for 20 min at 1,000 rpm to remove excess of extract. The supernatant was filtered through a membrane filter (0.45 µm) then 1 ml filtrate was diluted with 9 ml of distilled water or n-octanol and these samples were measured spectrometrically at 268 nm using UV spectrophotometer.<sup>29-30</sup>

#### **Entrapment efficiency**

Entrapment efficiency (EE) was measured using

$$EE (\%) = T-S/T \times 100$$

Where, T- Total concentration of SCL, S- SCL contained in the filtrate.

#### **Particle size distribution**

The particle size analysis of the prepared CP samples was carried out using photon correlation spectroscopy, with dynamic light scattering on Zetasizer nano (Model: Nano series, S90 Zeta sizer, Malvern). The CP was dispersed in isopropyl alcohol by stirring on a magnetic stirrer for 10 minutes. The dispersion was analyzed in size analyzer.

#### **X-Ray diffraction (XRD) study**

The crystalline state of samples (SCL, PC and CP) was evaluated with X ray powder diffraction. The diffraction patterns were obtained on powder X-ray diffractometer (D8 Advance Bruker, USA). The operating conditions were: voltage 45 kV; current 0.8 mA; scanning speed 1/min. The samples were scanned with the diffraction angle over a range of 5–60° (2θ angle), using the Cu-Anode X-ray tube and scintillation detector.

#### **Differential scanning calorimetry (DSC)**

The thermal analyses of samples (SCL, PC and CP) were carried out using differential scanning calorimeter Perkin Elmer (USA) (Model JADE

UV-visible spectrophotometer (UV-1601, Shimadzu). A weighed quantity of phyto-phospholipid complex (CP) equivalent to 10 mg was added to 50 ml methanol in a 100 ml beaker. The contents were stirred on a magnetic stirrer for 4 hours and then allowed to stand for one hour. Clear liquid was decanted and centrifuged at 5000 rpm for 15 minutes. After centrifugation the supernatant was filtered through 0.45 µm whatman filter paper and after suitable dilution absorbance was measured in UV at 268 nm; the concentration of drug was measured.<sup>31</sup> All measurements were performed in triplicate. The EE (%) was calculated using the following formula:

DSC). The analysis was performed under a purge of dry nitrogen gas. High-purity medium was used to calibrate the heat flow and the heat capacity of the instrument. The samples (~5 mg) were held in closed metal pans. Each sample was subjected to a single heating cycle from 0°C to 300°C at a heating rate of 10°C/min.

#### **Fourier Transform Infrared spectroscopy (FTIR) Study**

Fourier transform infrared spectrophotometer (Model: IR Prestige-21, Shimadzu, Japan) was employed to study the interaction between SCL and PC and to establish the structure and chemical stability of prepared CP, PC, and SCL. The IR spectra of CP, PC, and SCL were obtained by the potassium bromide (KBr) method. KBr pellets were prepared by gently mixing 1 mg sample with 100 mg KBr. A small quantity of sample was placed just below the probe on to which the probe was tightly fixed and scanned in the wave number region 4000-500 cm<sup>-1</sup>. The obtained IR spectra were interpreted for functional groups at their respective wave number (cm<sup>-1</sup>).

#### **Scanning electron microscopy (SEM)**

CP and SCL were coated with gold in a Fine Coat Ion Sputter (S-4800 TYPE II, Hitachi, Japan).

Analysis was done on the coated sample by placing a pinch of sample in the Scanning electron microscope and surface morphology was viewed and photographed to observe their particle shape and surface morphology.

### **Dissolution Study (In-Vitro Drug Release)**

The *in vitro* dissolution profiles of SCL, the PM, and the prepared CP were obtained.<sup>32</sup> The dissolution studies were carried out in a USP XXIII, six station dissolution test apparatus, type II (VEEGO Model No. 6 DR, India) at 100 rpm and at 37°C. An accurately weighed amount of CP of SCL 50 mg was put into 900 ml of pH 6.8 phosphate buffer. Samples (3 mL each) of dissolution fluid were withdrawn at different time intervals and replaced with an equal volume of fresh medium to maintain sink conditions. Withdrawn samples were filtered (through a 0.45 µm membrane filter), diluted suitably and then analyzed

spectrophotometrically at 268 nm to determine drug release from the complex and the drug.

### **Method for determination of in-vitro antioxidant activity**

#### **DPPH assay**

A methanolic solution of test sample was prepared at various concentrations (100-1000 µg/ml). To a set of test tubes, 2.9 ml of DPPH solution (100µg/ml in methanol) and 0.1 ml of varying concentrations of test sample were added. The mixture was then shaken vigorously and allowed to stand in dark for 30 min; absorbance at 517 nm was measured using a spectrophotometer. A control solution was consisting of 0.1 ml of methanol and 2.9 ml of DPPH radical solution.<sup>33</sup> Percentage scavenging of DPPH radical was calculated by comparing the absorbance between the test, mixture and control. % scavenging of DPPH radical was calculated by the formula,

$$\% \text{ Scavenging of DPPH} = \frac{\text{Absorbance (control)} - \text{Absorbance (sample)}}{\text{Absorbance (Control)}} \times 100$$

#### **Reducing power**

The reducing power of the SCL, PM, CP and vit C were determined according to the conventional method. Various concentrations of the extracts (100- 1000 µg/ ml) in 1.0 ml of deionized water were mixed with phosphate buffer (2.5 ml, 0.2M, pH 6.6) and 1% potassium ferricyanide (2.5 ml). The mixture was incubated at 50°C for 20 min. Aliquots of trichloroacetic acid (2.5 ml, 10%) were added to the mixture, which was then centrifuged at 3000 rpm for 10 min. The upper layer of solution (2.5 ml) was mixed with distilled water (2.5 ml) and a freshly prepared ferric chloride solution (0.5 ml, 1%). The absorbance was measured at 700 nm. Increased absorbance of the reaction mixture indicated increased reducing power.<sup>34</sup>

## **STATISTICAL ANALYSIS**

The results are presented as mean ± standard deviation. The statistical analysis was carried out using one-way analysis of variance (ANOVA)

followed by Student's t-test. P values < 0.05 were assumed as statistically significant.

## **RESULT AND DISCUSSION**

### **Preparation of CP**

The preliminary investigation of the influence of factors revealed that all the tested variables, i.e., the phospholipid to drug ratio, the reaction temperature, and the reaction time had a significant influence on the entrapment efficiency of the prepared phytosome. The results of the entrapment efficiency (%) are shown in Table 2. The measured values from the experimental trials revealed wide range (58.16–96.24 %w/w) entrapment efficiencies (Table 2). A mathematical relationship between factors and parameters was generated by response surface regression analysis in the software Minitab 17. The three-dimensional response surface plots for the most statistically significant variables on the evaluated responses are shown in Figure 1. The equations represent the quantitative effect of process variables ( $X_1$ ,  $X_2$ , and  $X_3$ ), and their interactions on response Y are as follows:

$$Y = 90.48 + 7.94 X_1 + 2.63 X_2 + 5.45 X_3 - 4.601 X_1^2 - 1.773 X_2^2 - 1.632 X_3^2 + 1.87 X_1 X_2 - 3.47 X_1 X_3 + 1.60 X_2 X_3$$

The polynomial model for Y was found to be significant, with F values of 14.88 (P<0.05). The value of correlation coefficient ( $R^2$ ) was found to be 0.9305, indicating a good fit to the quadratic

model. The multiple regression analysis revealed that the coefficients  $b_1$ ,  $b_2$ , and  $b_3$  were positive. Based on the central composite design, the response surface plots show the changes in the entrapment

efficiency (%) as a function of  $X_1$ ,  $X_2$ , and  $X_3$ . The data from all 20 batches of the central composite design were used for generating interpolated values using software. The response surface plots indicated a strong influence of the studied factors  $X_1$ ,  $X_2$ , and  $X_3$  on the entrapment efficiency (Figure 1). Increasing levels of  $X_1$ ,  $X_2$ , and  $X_3$  were found

to be favorable conditions for obtaining higher entrapment efficiency. Based on these observations, the optimal values of the studied factors, i.e., the phospholipids-to-drug ratio, the reaction temperature, and the reaction time were 3:1, 65°C, and 2 h, respectively.

**Table 2**  
*Central composite design formulation batches*

Formulation	$X_1$	$X_2$	$X_3$	Entrapment efficiency <sup>a</sup> (% w/w)
1	-1	-1	-1	64.72±1.5
2	1	-1	-1	82.21±0.3
3	-1	1	-1	71.51±1.6
4	1	1	-1	90.36±0.9
5	-1	-1	1	89.52±1.3
6	1	-1	1	86.41±1.1
7	-1	1	1	83.23±1.2
8	1	1	1	94.32±1.4
9	-1.68	0	0	58.16±1.0
10	1.68	0	0	96.24±0.9
11	0	-1.68	0	79.42±1.7
12	0	1.68	0	90.93±1.2
13	0	0	-1.68	76.72±0.8
14	0	0	1.68	94.45±1.4
15-20	0	0	0	90.51±0.9

<sup>a</sup>Values represent mean ± standard deviation (n=3)

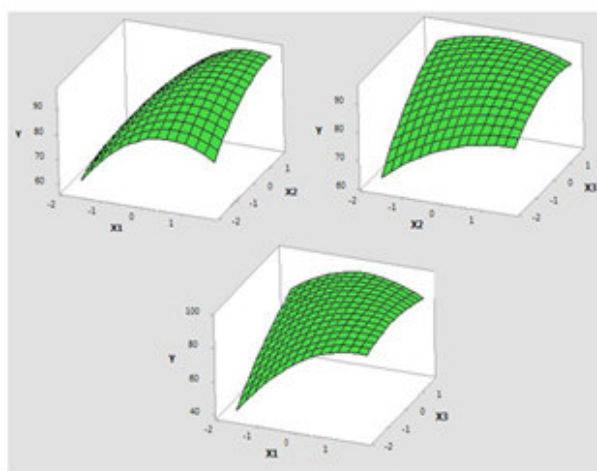


**Figure 1**

*Response surface plot showing the influence of phospholipids-drug ratio ( $X_1$ , w/w), the reaction temperature ( $X_2$ , °C), and the reaction time ( $X_3$ , h) on entrapment efficiency of SCL*

#### **Validation of optimized model**

An additional batch of CP was prepared in order to evaluate the optimization capability of the models generated according to the result of central composite design-response surface methodology

using the optimized values of the variables, i.e.  $X_1$ ,  $X_2$ , and  $X_3$  3:1, 65°C, and 2 h, respectively. A comparison between the predicted (theoretical) value (%) of the CP obtained from the developed model and the observed value (%) achieved from

the prepared formulation was carried out. The model-predicted value for the entrapment efficiency of SCL in CP was 98.99%, while the average observed value (%) from the prepared batches was found to be 97.19 %, indicating both applicability,

and validity of the developed model. The bias (%), calculated using the equation, was also found to be less than 3% (1.8%), indicating the relative robustness of the model.

$$\text{Bias (\%)} = \frac{\text{predicted value} - \text{observed value}}{\text{predicted value}} \times 100$$

**Table 3**  
*Observed and Predicted value of entrapment efficiency prepared under optimal protocol*

Batches	Predicted value (%)	Observed value (%) <sup>a</sup>	Bias
1	98.99	97.51±0.32	1.48
2	98.99	98.87±1.12	0.12
3	98.99	95.19±0.24	2.8

<sup>a</sup>All values are mean ± SD (n=3)

#### *Physico-chemical characterization of prepared CP*

##### *Apparent Solubility of CP*

The apparent solubility of the pure SCL, the physical mixture of SCL and PC, and the prepared SCL-PC complex (CP) are shown in Table 3. It was observed that the pure SCL had poor aqueous solubility (2.35 µg/mL), and a relatively higher solubility in n-Octanol (305 µg/mL). The physical

mixture (PM) enhanced the solubility of SCL but this effect was weaker. The prepared CP showed a significant increase in the aqueous solubility. This increase in the solubility of the prepared complex may be explained by reduced molecular crystallinity of the drug and the overall amphiphilic nature of the phytosome.<sup>35-36</sup>

**Table 4**  
*Apparent solubility study of SCL, PM and CP in water and n-octanol*

SN	Sample	Aqueous Solubility (µg/mL) <sup>a</sup>	n-Octanol solubility (µg/mL) <sup>a</sup>
1	SCL	2.35 ± 0.34	305.65 ± 0.54
2	PM	8.12 ± 1.35	432.21± 0.04
3	CP	80.32 ± 0.13	617.34 ±0.58

<sup>a</sup>All values are mean ± SD (n=3)

##### *Particle size distribution*

The particle size of the prepared CP was carried out using dynamic light scattering technique. The mean particle size of CP was distributed in a narrow range of 233.4 ± 20.0 nm, and polydispersity index was 0.642 ± 0.03 (Figure 2). The surface area to volume (SA/V) ratio of most particles is inversely

proportional to the particle size. Thus, smaller particles of the CP, having a higher SA/V, make it easier for the entrapped drug to be released from the phytosome via diffusion and surface erosion. They have the advantage for the drug entrapped phytosomes to penetrate into, and permeate through the physiological drug barriers.<sup>37-39</sup>

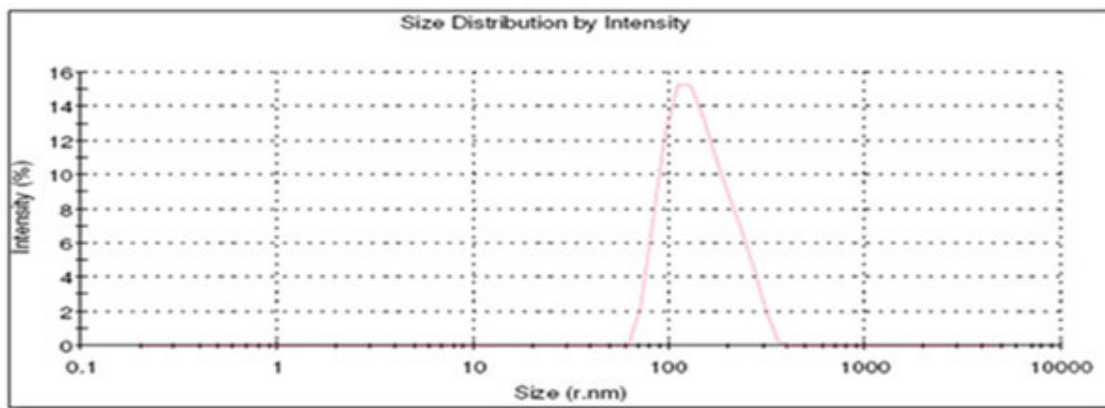


**Figure 2**  
*Particle size analysis of CP*

### *X-Ray diffraction (XRD) study*

The powder x-ray diffraction (PXRD) patterns of (A) SCL, (B) PC, (C) PM, and (D) CP are shown in figure 3. SCL (Figure 3A) revealed sharp crystalline peaks at  $2\theta=46.9^\circ$ ,  $43.5^\circ$ ,  $36.6^\circ$ , and  $28.0^\circ$ . A diffraction peak was observed for PC at  $35.5^\circ$ ,  $36.4^\circ$ , and  $25.2^\circ$ . The physical mixture (PM) showed most of the peaks associated with the SCL and PC (Figure 3C). The diffractogram of the CP

revealed the disappearance of most of the crystalline peaks associated with the SCL and when compared with physical mixture (PM). These results were in concord with reported studies, where the disappearance of the API peaks was associated with the formation of drug phospholipid complex.<sup>40</sup> The disappearance of SCL crystalline peak confirms the formation of SCL-phospholipid complex.

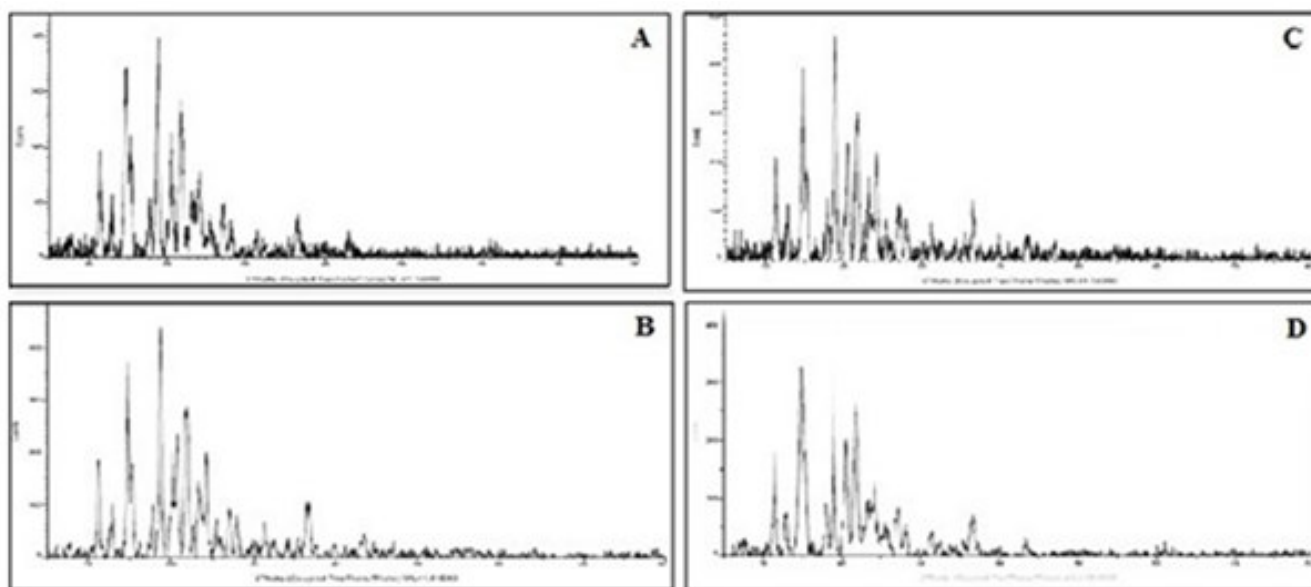


**Figure 3**  
*XRD spectra of (A) SCL, (B) PC, (C) PM and (D) CP*

### *Scanning electron microscopy (SEM)*

SEM photographs of SCL and CP are shown in figure 4. Crystalline state of SCL was visualized in the SEM photograph as numerous crystals in figure 4 (A). In figure 4 (B) the drug was completely

converted into phyto-phospholipid (CP) complex where SCL was physically wrapped by phospholipid imparting amorphous nature to the complex due to which crystals disappeared.

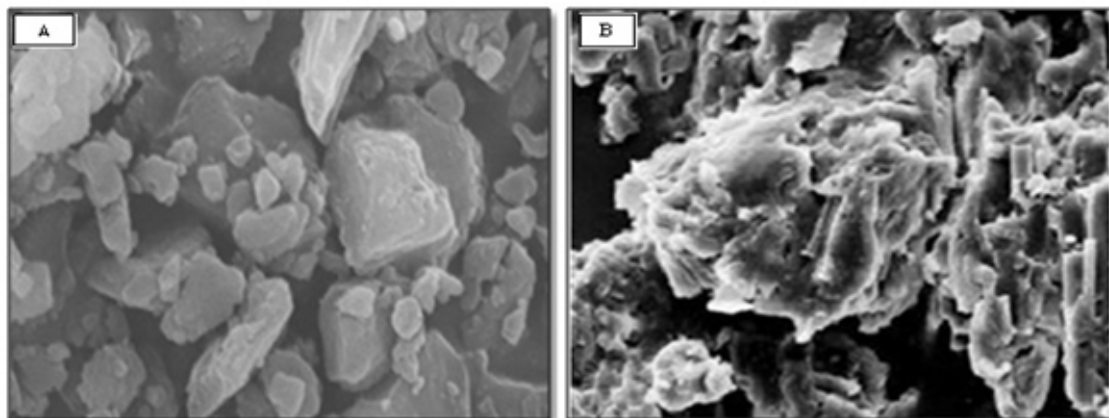


**Figure 4**  
**SEM of SCL (A) and CP (B)**

#### **FT-IR study**

Fourier transform infrared spectroscopy (FTIR) analyses of the SCL, PC, the physical mixture of SCL with PC (PM), and the prepared CP were studied interaction between SCL and PC. The FTIR spectrum of SCL showed broad peak at  $3556\text{ cm}^{-1}$  representing the aliphatic alcoholic ( $-\text{OH}$ ) group,  $2900\text{ cm}^{-1}$  (CH stretching),  $1660\text{ cm}^{-1}$  ( $\text{C}=\text{O}$  stretching),  $1559\text{ cm}^{-1}$  ( $\text{C}=\text{C}$  stretching). Prominent peak observed at  $1160\text{ cm}^{-1}$  and  $1050\text{ cm}^{-1}$  typically relates to the presence of acidic functional group. FTIR spectrum of PC (Figure 5B) revealed

the characteristic absorption at  $2921$  and  $2850\text{ cm}^{-1}$  (CH stretching),  $1775\text{ cm}^{-1}$  ( $\text{C}=\text{O}$  stretching),  $1235\text{ cm}^{-1}$  ( $\text{P}=\text{O}$  stretching),  $1081\text{ cm}^{-1}$  ( $\text{P}-\text{O}-\text{C}$  stretching) and  $975\text{ cm}^{-1}$  ( $\text{C}-\text{C}-\text{N}$  stretching). The FTIR spectrum of the prepared CP (Figure 5D) is quite different from that of SCL and PC. The peaks at  $1660\text{ cm}^{-1}$ ,  $1559\text{ cm}^{-1}$  and  $3556\text{ cm}^{-1}$  were shielded by phospholipids. The absorption at  $1660\text{ cm}^{-1}$  shifted to lower field in the spectrum of complex, indicating the formation of hydrogen bond and existence electrostatic interaction between extract and phospholipid.<sup>41</sup>

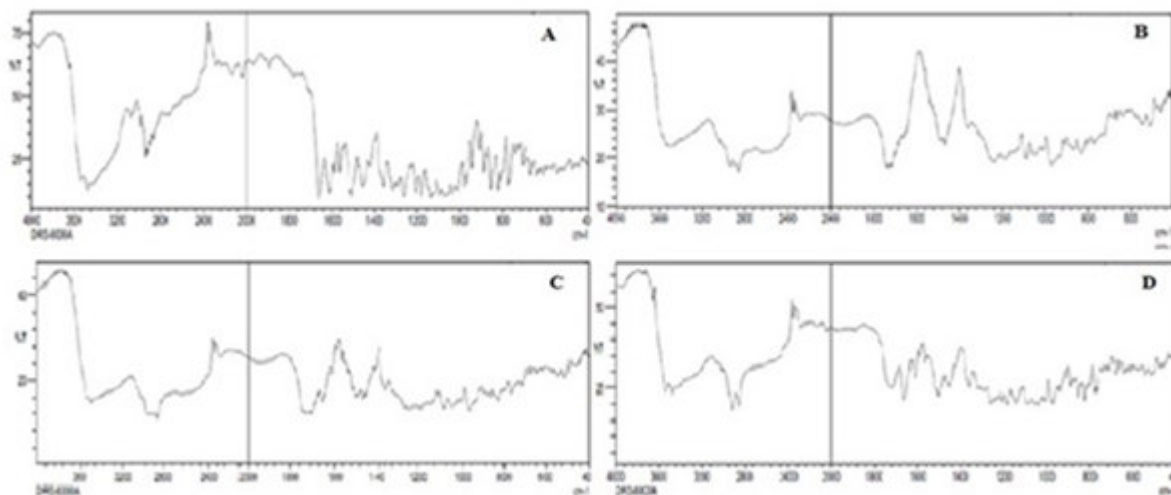


**Figure 5**  
**FTIR spectra of (A) SCL, (B) PC, (C) Physical mixture and (D) CP**

#### **Differential scanning calorimetry (DSC)**

DSC is a fast, reliable method to investigate the interaction between multiple component and drug excipient compatibility. These interactions are observed as the elimination of endothermic peak, the appearance of new peak, the change in peak shape, onset temperature/ melting point, relative peak area or enthalpy.<sup>42-43</sup> The SCL revealed broad

endothermic peaks at  $126.48^{\circ}\text{C}$  and  $272.79^{\circ}\text{C}$ . The DSC thermogram of CP showed figure 6 B gives two endothermic peaks at  $206.40^{\circ}\text{C}$  and  $244.54^{\circ}\text{C}$ . Therefore from figure 6 it was revealed that the shift of endothermic peak at the difference of around  $25-30^{\circ}\text{C}$  suggest possible interaction of SCL with PC and can account for enhanced entrapment.



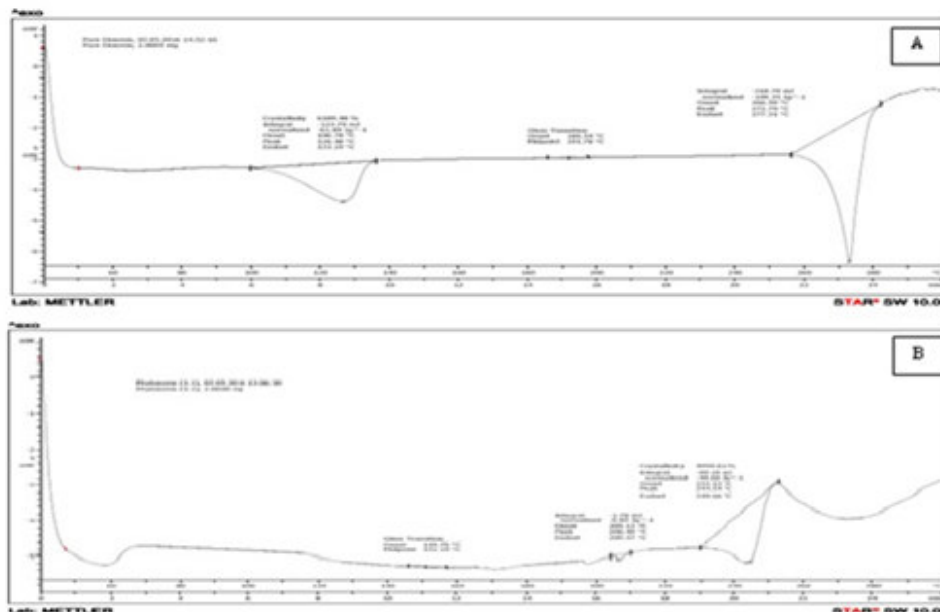
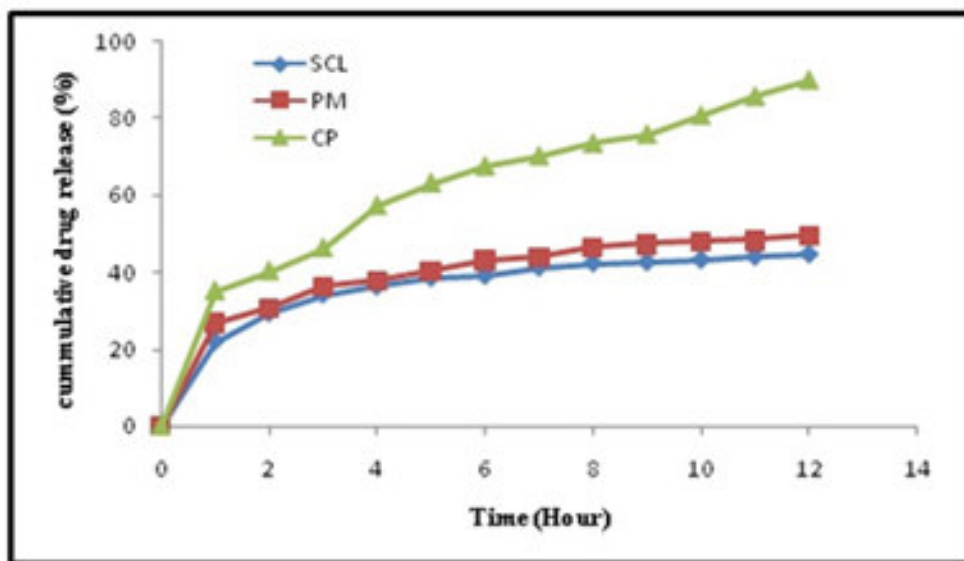


**Figure 6**  
*Differential scanning Calorimetry of (A) SCL and (B) CP*

**Percentage drug release**

The results of in vitro drug release studies are shown in graph 1. The 12-h dissolution in the phosphate buffer (pH 6.8) revealed that, the pure SCL showed the slowest rate of dissolution, i.e., at the end of the dissolution period only about 44% w/w of SCE was dissolved. The dissolution rate of the physical mixture was found not to be significantly different (49% w/w dissolved in 12 h) compared to the pure SCL. The prepared CP revealed a significantly faster release of SCL at the

end of dissolution period. At the end of 12 h, over 89% w/w SCL was observed to be released from the CP. The dissolution rate is largely influenced by the crystal morphology and the wettability of the solids,<sup>44</sup> and the improved dissolution rate of SCL from the CP may be explained by the improved solubility, and the amorphous form in the prepared complex. The relatively higher amorphous state of the phytosome and the increased aqueous solubility may have a positive impact on the cumulative release of the drug.<sup>45</sup>



**Graph 1**  
*In vitro* dissolution study of SCL, PM and CP

### Assessment of antioxidant activity

The extracts were capable of scavenging free radical and inhibiting DPPH in a concentration dependent manner. DPPH has been widely used to evaluate the free radical scavenging effect of various antioxidant substances. In the DPPH assay, the antioxidants are able to reduce the stable radical DPPH to the yellow coloured diphenyl-picryl hydrazine. DPPH is used as a reagent to evaluate free radical scavenging activity of antioxidants. DPPH is a stable free radical and accepts an electron or hydrogen radical to become a stable diamagnetic molecule.<sup>46</sup> With this method it was possible to determine the antiradical power of an antioxidant by measuring the absorbance of DPPH. The % scavenging effect of on the DPPH radical increase as the concentration of CP, SCL and vitamin C is increase in the order of vitamin C > SCL > CP, which were 95.56%, 94.74% and 70.08%, at the concentration of 1000 µg/mL, respectively (Graph 2). IC 50 is often used to express the amount or concentration of extracts needed to scavenge 50% of the free radicals. The IC50 value is inversely proportional to the scavenging activity of the extract. The anti-oxidant

activity of the extract was expressed as (IC 50), which was defined as the concentration (µgml<sup>-1</sup>) of extract required to scavenge 50% of radicals. The IC 50 of CP was 311.91 µgml<sup>-1</sup> in comparison to standard ascorbic acid 274.32 (Table 5). Reducing power is associated with antioxidant activity and may serve as significant reflection of the antioxidant activity. Compounds with reducing power indicate that they are electron donors, so that they can act as primary and secondary antioxidants. The reducing capacity of a plant is much related to the presence of biologically active compounds with potent donating abilities.<sup>47</sup> The reducing power assay is used to test the reducing capability of standardised extract SCL and phytosome CP to convert the potassium ferricyanide (Fe<sup>3+</sup>) complex to form potassium ferrocyanide (Fe<sup>2+</sup>). The potassium ferrocyanide will then react with ferric chloride to form ferrous complex which can absorb maximally at 700 nm. Graph 3 shows pattern of increment in reducing power with increase in concentration of SCL, CP and vitamin C. Higher absorbance of the reaction mixture indicates higher reductive potential.<sup>48</sup>

**Table 5**  
*DPPH radical scavenging activity of extract*

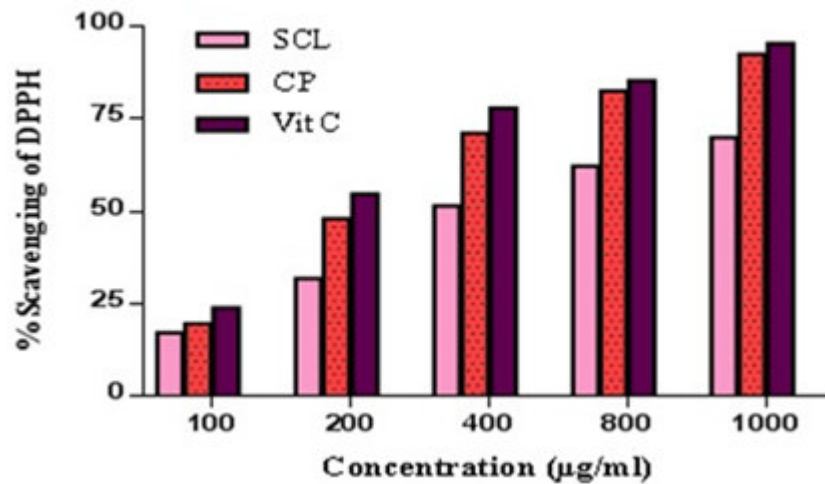
	Concentration µg/ml and % scavenging of DPPH*					IC 50
	100	200	400	800	1000	
1. SCL	17.21±0.16	31.86±1.31	51.57±0.67	62.32±1.02	70.08±0.22	387.82±0.52
2. CP	19.70±1.23	48.09±0.43	71.18±1.21	82.62±1.32	94.74±1.42	311.91±1.32
3. Vit C	23.92±0.13	54.68±0.21	78.04±1.16	85.34±0.46	95.56±1.26	274.32±0.91

\* All values are mean ± SD (n=3)

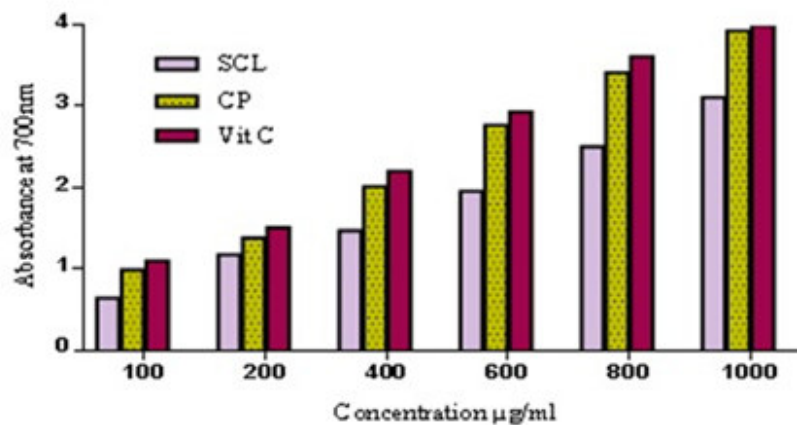
**Table 6**  
*Reducing power of sample*

	Concentration µg/ml and Absorbance at 700 nm*					
	100	200	400	600	800	1000
1. SCL	0.64±1.52	1.17±1.02	1.47±1.03	1.95±0.02	2.50±1.2	3.11±1.82
2. CP	0.98±0.12	1.38±0.12	2.01±0.32	2.76±0.8	3.41±1.0	3.93±0.15
3. Vit C	1.09±1.81	1.50±0.54	2.20±0.89	2.93±1.9	3.61±0.9	3.99±1.02

\* All values are mean ± SD (n=3)



**Graph 2**  
*DPPH radical scavenging activity of SCL and CP*



**Graph 3**  
*Reducing powers of SCL and CP*

## CONCLUSIONS

An attempt was made to enhance the solubility of SCL by its complexation with phospholipids. A central composite design-response surface methodology was used to optimize the formulation. The prepared phytosome (CP) was characterized by FTIR, DSC, PXRD, photo microscopy, and the SEM. These studies indicated the successful formation of vesicular drug-phospholipids complex.

## REFERENCES

1. Campelo LML, Almeida AAC, Freitas RLM. Antioxidant and antiniociceptive effects of *Citrus limon* essential oil in mice. *J Biomed Biotech.* 2011; 1-8.
2. Trovato A, Monforte MT, Barbera R, Rossitto A, Galati EM and Forestieri AM, Effects of fruit juices of *Citrus sinensis* and

The apparent solubility and *in vitro* dissolution studies indicated a significant improvement in the solubility and the drug release of SCL from CP respectively. The *in vitro* evaluation revealed a significantly higher antioxidant activity of the prepared CP compared to the pure SCL.

## CONFLICT OF INTEREST

Conflict of interest declared none.

3. Kawaii ST, Yasuhiko KE, Kazunori O, Masamichi Y, Meisaku K, Chihiro I and Hiroshi F. Quantitative study of flavonoids in leaves of *Citrus* plants. *J Agric Food Chem.* 2000; 48: 3865-71.

4. Duthie G and Crozier A. Plant-derived phenolic antioxidants. *Curr Opin Lipidol.* 2000; 11: 43-47.
5. Greenish HG. *Materia Medica.* Scientific publishers. 1999; 3: 92-94.
6. Jaiswal SK, Gupta VK, Siddiqi NJ, Pandey RS and Sharma B. Hepatoprotective Effect of *Citrus limon* Fruit Extract against Carbofuran Induced Toxicity in Wistar Rats Chinese.. *J Biol.* 2015; 1-10.
7. Pashazanousi MB, Raeesi M and Shirali S. Chemical composition of the Essential oil, antibacterial and antioxidant activities, total phenolic and flavonoid evaluation of various extracts from leaves and fruit peels of *Citrus limon*. *Asian J Chem.* . 2012; 24(10): 4331-34.
8. Mohanapriya M, Ramaswamy L, Rajendran R. Health and Medicinal Properties of Lemon (*Citrus Limonum*). *Int J Ayu Herbal Med.* 2013; 3(1): 1095-1100.
9. Kumar S and Pandey AK. Chemistry and Biological Activities of Flavonoids: An Overview. *Scient World J.* 2013; 1-16.
10. Manthey JA. Biological properties of flavonoids pertaining to inflammation. *Microcirculation.* 2000; 7(6): 29-34.
11. Abourashed EA. Bioavailability of Plant-Derived Antioxidants. *Antioxidants.* 2013; 2: 309-325.
12. Zenovia M, Andrei AB, Mohammed AA, Hassan YA. A Spectrophotometric Method for Diosmin Determination. *Open Chem Biomed Method J.* 2010; 3: 123-7.
13. Diosmin monograph, *Alt Med Review.* 2004; 9(3): 308-11.
14. Chebil L, Humeau C, Anthoni J, Dehez F, Engasser JM, Ghoul M. Solubility of flavonoid in organic solvents. *J Chem Eng data.* 2007; 52: 1552-6.
15. Freag MS, Elnaggar YSR, Abdallah OY. Lyophilized phytosomal nanocarriers as platforms for enhanced diosmin delivery: optimization and ex vivo permeation. *Int J Nanomed.* 2013; 8: 2385-97.
16. Nagasamy VD, Sumanraj S, Saicharithach, Karri T. Phytosomes- a review. *Int J Pharm Sci.* 2014; 4: 622-25.
17. Acharya NS, Parihar GV, Acharya SR. Phytosomes: novel approach for delivering herbal extract with improved bioavailability. *Int J Phram Sci.* 2011; 2(1): 144-60.
18. Tawheed A, Bhat SV. A Review on Phytosome Technology as a Novel approach to improve the Bioavailability of Nutraceuticals. *Int J Adv Res Tech.* 2012; 3(1): 1-15.
19. Udupurkar P, Bhusnure O, Kamble S, Biyani K. Phyto-phospholipid complex vesicles for phytoconstituents and herbal extracts: A promising drug delivery system. *Int J Herb Med.* 2016; 4(5): 14-20.
20. Semalty A, Semalty M, Singh M, Rawat M, Franceschi F. Supramolecular phospholipids –polyphenolics interactions: The PHYTOSOME® strategy to improve the bioavailability of phytochemicals. *Fitoterapia.* 2010; 8: 306–314.
21. Jing Li, Xuling Wang, Ting Zhang, Chunling Wang, Zhenjun Huang, Xiang Luo, Yihui Deng. A review on phospholipids and their main applications in drug delivery systems. *Asian J Pharm Sci* 2015; 10: 81-98.
22. Scholfield CR. Composition of soybean lecithin. *J Amer Oil Chem Socie..* 1998; 58(10): 889-92.
23. Bombardelli E, Curri SB, Della LR, Del Negro P, Tubaro A, Gariboldi P. Complex between phospholipids and vegetable derivatives of biological interest. *Fitoterapia.* 1989; 60: 1-9.
24. Lei L, Daniel LEW, Terry JR, Jinsong B, Graham JK. Phospholipids in rice: Significance in grain quality and health benefits: A review. *Food Chemistry.* 2013; 139(1-4): 1133-45.
25. Parris MK. Bioavailability and Activity of Phytosome Complexes from Botanical Polyphenols: The Silymarin, Curcumin, Green Tea, and Grape Seed Extracts. *Alt Med Rev.* 2009; 14(3): 226-46.
26. Malay KD, Bhupen K. Design and Evaluation of Phyto-Phospholipid Complexes (Phytosomes) of Rutin for Transdermal Application. *Journal of Applied Pharmaceutical Science.* 2014; 4 (10): 51-7.
27. Qunyou T, Shan L, Xueliang C, Mingjun W, Hong W, Huafeng Y, Dan H, Huarong X, Jingqing Z. Design and Evaluation of a Novel Evodiamine-Phospholipid Complex for Improved Oral Bioavailability. *AAPS Pharm SciTech.* 2012; 13(2): 534-47.
28. Xuan Q, Yang Y, Ting TF, Tao G, Xiaoning Z, Yuan H. Preparation, Characterization and *in vivo* evaluation of bergenin-phospholipid complex. *Acta pharmacol sinica* 2010; 31: 127–36.
29. Devendra SR, Bandana KT, Semalty M, Semalty A, Badoni P, Rawat MSM, Baicalein-Phospholipid Complex: A Novel

- Drug Delivery Technology for Phytotherapeutics. *Curr Drug Disc Tech.* 2013; 10(3): 1-9.
30. Xiaoqing C, Yuxia L, Yue J, Aixin S, Wei S, Zhonghao L, Zhongxi Z. Huperzine A-phospholipid complex-loaded biodegradable thermosensitive polymer gel for controlled drug release. *Int J Pharm.* 2012; 433: 102–11.
31. Damle M, Mallya R. Development and Evaluation of a Novel Delivery System Containing Phytophospholipid Complex for Skin Aging. *AAPS Pharm Sci Tech.* 2016; 17(3): 607-17.
32. Saoji SD, Belgamwar VS, Dharashivkar SS, Rode AA, Mack C, Dave VS. The Study of the Influence of Formulation and Process Variables on the Functional Attributes of Simvastatin-Phospholipid Complex. *J Pharm Innov.* 2016; 1-15.
33. Sahu AN. Development And Characterization Of Hepatoprotective Phytosomes Of *Abutilon Indicum* And *Piper Longum*. *Int J Pham Biol Sci.* 2015; 5(4): 97-106.
34. Jayanthi P, Lalitha P. Reducing power of the solvent extracts of *Eichhornia Crassipes*. *Int J Pharm sci.* 2011; 3(3): 126-8.
35. Shrestha H, Bala R, Arora S. Lipid-Based Drug Delivery Systems. *J Pharma.* 2014; 1-10.
36. Sovova H. Apparent Solubility of Natural Products Extracted with Near-Critical Carbon Dioxide. *Amer J Anal Chem.* 2012; 3: 958-65.
37. LeFevre ME, Olivo R, Vanderhoff JW, Joel DD. Accumulation of latex in Peyer's patches and its subsequent appearance in villi and mesenteric lymph nodes. *Proc Soc Exp Biol Med.* 1978; 159(2): 298–302.
38. Savic R, Luo L, Eisenberg A, Maysinger D. Micellarnanocontainers distribute to defined cytoplasmic organelles. *Science.* 2003; 300(5619): 615–8.
39. Freitas C, Müller RH. Effect of light and temperature on zeta potential and physical stability in solid lipid nanoparticle (SLN™) dispersions. *Int J Pharm.* 1998; 168(2): 221–9.
40. Jena SK, Singh C, Dora CP, Suresh S. Development of tamoxifen-phospholipid complex: novel approach for improving solubility and bioavailability. *Int J Pharm.* 2014; 473(1–2): 1–9.
41. Singh C, Bhatt TD, Gill MS, Suresh S. Novel rifampicin phospholipid complex for tubercular therapy: synthesis, physicochemical characterization and in-vivo evaluation. *Int J Pharm.* 2014; 460(1–2): 220–7.
42. Hai-jian X, Zhen-hai Z, Xin J, Qin H, Xiao C, Xiao-bin J, A novel drug-phospholipid complex enriched with micelles: preparation and evaluation in vitro and in vivo. *Int J Nanomed.* 2013; 8: 545–54.
43. Semalty A, Semalty M, Singh D, Rawat MSM. Phytophospholipid complex of catechin in value added herbal drug delivery. *J Incl Phenom Macrocycl Chem.* 2012; 73(1–4): 377–86.
44. Vora AK, Londhe VY, Pandita NS. Preparation and characterization of standardized pomegranate extract phospholipid complex as an effective drug delivery tool. *J Adv Pharm Tech Res.* 2015; 6(2): 75-80.
45. Kalita B, Das MK, Sarma M, Deka A. Skin targeted delivery of rutin-phospholipid complex: Patch formulation, *in vitro-in vivo* evaluation. *World J Pharm Sci.* 2015; 3(10): 2042-57.
46. Ilhami G, Zubeyr H, Mahfuz E, Hassan Y, Aboul E. Radical scavenging and antioxidant activity of tannic acid. *Arb J Chem.* 2010; 3: 43–53.
47. Seow-Mun H, Amru NB, Chandran S. Antioxidant activity, phenolic and flavonoid contents in the leaves of different varieties of sweet potato (*Ipomoea batatas*). *AJCS.* 2012; 6(3): 375-80.
48. Md NA, Bristi NJ, Md R. Review on *in vivo* and *in vitro* methods evaluation of antioxidant activity. *Saudi Pharm J.* 2013; 21: 143–52.